Inorganic Chemistry

ARTICLE

pubs.acs.org/IC

Probing the Structural Origins of Vapochromism of a Triarylboron-Functionalized Platinum(II) Acetylide by Optical and Multinuclear Solid-State NMR Spectroscopy

Zachary M. Hudson,[†] Christina Sun,[†] Kristopher J. Harris,[‡] Bryan E. G. Lucier,[‡] Robert W. Schurko,*[,‡] and Suning Wang*[,†]

[†]Department of Chemistry, Queen's University, 90 Bader Lane, Kingston, Ontario, Canada K7L 3N6

[‡]Department of Chemistry & Biochemistry, University of Windsor, 401 Sunset Avenue, Windsor, Ontario, Canada N9B 3P4

Supporting Information

ABSTRACT: A vapoluminescent triarylboron-functionalized platinum(II) complex that displays a mechanism of vapochromism differing from all previously reported platinum(II) compounds has been synthesized. The luminescence color of **1** switches in response to many volatile organic compounds in the solid state, including hexanes, CH_2Cl_2, benzene, and methanol. While vapochromism due to changes in Pt—Pt or π—π stacking interactions has been commonly observed, absorption and luminescence studies and single-crystal and powder X-ray diffraction data as well as multinuclear solid-state NMR experiments (^{195}Pt, ^{13}C, ^{11}B, ^{2}H, and ^{1}H) revealed that the vapochromic response of **1** is instead due to changes in the excited-state energy levels resulting from local interactions of solvent molecules with the complex. Furthermore, these interactions result in inversion of the lowest-energy excited states of the complex in some cases, the first observation of this phenomenon in the solid state.

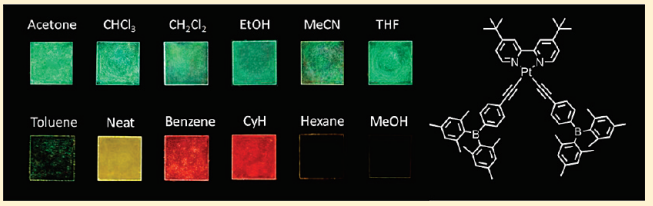

INTRODUCTION

There has been considerable interest in recent years in the development of vapochromic sensor materials for the detection of volatile organic compounds (VOCs).[1−3] Such materials reversibly show changes in absorption and/or luminescence color upon exposure to VOCs and are attractive because of their ability to provide a highly sensitive and rapid response to volatile contaminants, as well as their potential for use in portable fiber-optic devices.[3c,d,4] Vapochromic materials based on gold(I) [Au(I)][3] and platinum(II) [Pt(II)][1,2a−2h] are the most extensively investigated and usually take advantage of metal—metal or metallophilic interactions in the solid state. The enhancement or disruption of this interaction upon adsorption of VOCs can thereby alter the highest occupied molecular orbital (HOMO)—lowest unoccupied molecular orbital (LUMO) gap, leading to distinct absorption or emission color changes. Vapochromic systems have also been investigated based on the reversible binding of an analyte such as SO_2 to a fifth coordination site of Pt(II).[2g] Furthermore, flexible coordination polymers based on a Pt(II) scaffold have proven useful in host—guest sensing applications as well.[2i]

Luminescent materials based on triarylboranes have also been the focus of much recent research activity, although until now toward entirely different applications. Because of the electron-accepting empty p_π orbital on the boron center, these compounds have been developed into a wide range of functional materials.[5] These include highly efficient luminescent and electron-transport materials for organic light-emitting diodes,[6] compounds with nonlinear optical properties,[7] and highly sensitive and selective chemical sensors for fluoride and cyanide.[8] Furthermore, the triarylboron group has recently been shown to greatly enhance metal-to-ligand charge-transfer (MLCT) phosphorescence in complexes of Pt(II) and iridium(III), making this functionality attractive for use in phosphorescent materials as well.[9]

Herein we report the first example of a vapochromic material based on triarylboron and Pt(II), which shows a distinct luminescent response to a wide variety of VOCs (**1** in Chart 1). Furthermore, extensive investigations into the structural origins of vapochromism in this system using optical and multinuclear solid-state ^{195}Pt, ^{13}C, ^{11}B, ^{2}H, and ^{1}H NMR spectroscopies have indicated that the mechanism of this vapochromic behavior arises not from differences in metallophilic or π—π stacking interactions but instead from modulations of the excited-state energy levels on individual molecules due to interactions with an adsorbed VOC analyte. We report herein the first comprehensive solid-state NMR study on a vapochromic material and demonstrate that the vapochromism of this material differs in origin from those of all previously reported examples.

EXPERIMENTAL SECTION

Reagents and Physical Characterization. All reagents were purchased from Sigma-Aldrich and used without further purification.

Received: November 24, 2010
Published: March 22, 2011

Chart 1

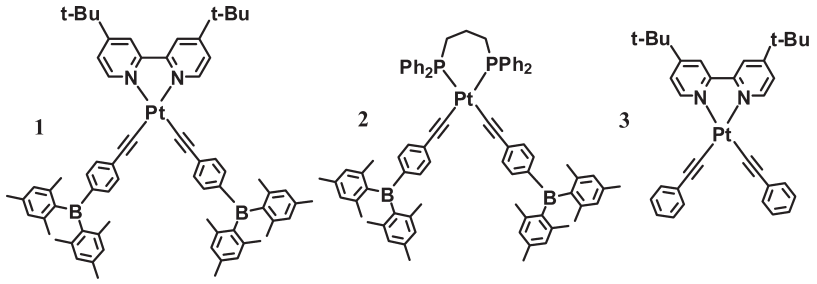

Thin-layer and flash chromatography were performed on silica gel. Solution ^{1}H and ^{13}C NMR spectra were recorded on a Bruker Avance 400, 500, or 600 MHz spectrometer. Deuterated solvents were purchased from Cambridge Isotopes and used without further drying. Excitation and emission spectra were recorded using a Photon Technologies International QuantaMaster model 2 spectrometer. UV/visible spectra were recorded using an Ocean Optics CHEMUSB4 absorbance spectrophotometer. Cyclic voltammetry (CV) experiments were performed using a BAS CV-50W analyzer with a scan rate of 0.2−1.0 V/s using 5 mg of the sample in 3 mL of dry *N*,*N*-dimethylformamide (DMF). The electrochemical cell was a standard three-compartment cell composed of a Pt working electrode, a Pt auxiliary electrode, and an Ag/AgCl reference electrode. CV measurements were carried out at room temperature with 0.1 M tetrabutylammonium hexafluorophosphate as the supporting electrolyte, with ferrocene/ferrocenium as the internal standard (E° = 0.55 V). Elemental analyses were performed by Canadian Microanalytical Service Ltd., Delta, British Columbia, Canada. Powder X-ray diffraction (PXRD) patterns were acquired using a Bruker D8 Discover diffractometer using Cu Kα radiation (λ = 1.540 56 Å); samples of **1** were exposed to the vapor of each solvent for a minimum of 8 h in a sealed chamber and then packed into glass capillaries, which were sealed with silicon grease. Photoluminescent quantum yields were measured using the optically dilute method ($A \approx 0.1$) at room temperature in degassed CH_2Cl_2 using *fac*-Ir(ppy)$_3$ in 2-methyltetrahydrofuran (2-MeTHF) as the standard (Φ_r = 0.97),[10] using the equation

$$\Phi_s = \Phi_r \frac{I_s A_r \eta_s^2}{I_r A_s \eta_r^2}$$

where Φ_s and Φ_r are the quantum yields of the sample and reference, I is the integrated area of the emission band, A is the absorbance at the wavelength of excitation, and η is the refractive index of the solvent. Samples for quantum yield measurement were prepared by bubbling dry N_2 through a quartz cuvette fitted with a rubber septum and then sealed with epoxy and measured immediately. Using this method, no loss of the emission intensity was observed after 5 min of standing under air, and <5% intensity loss was observed after 30 min. Vapor-dependent solid-state emission spectra were obtained by exposing a powdered film of **1** in a quartz cuvette to a drop of solvent vapor. Films of **1** were prepared by manually applying small amounts of powdered material to the quartz surface. Phosphorescent decay lifetimes were below the measurement limit for our instrument ($\leq$2 μs). Molecular orbital (MO) calculations were performed using the *Gaussian 03* program suite using crystal structures as the starting point for geometry optimizations where possible. The theoretical absorption spectrum of **1** was generated using the *Gausssum 2.1.6* software package.[11] Calculations were performed at the B3LYP level of theory using LANL2DZ as the basis set for Pt and 6-31G* for all other atoms.[12] Syntheses of *p*-(dimesitylboryl)phenylacetylene,[13] Pt(dbbpy)Cl$_2$ (dbbpy = 4,4′-di-*tert*-butyl-2,2′-bipyridine),[14] Pt(dppp)Cl$_2$ (dppp = 1,3-diphenylphosphinopropane),[15] and Pt(dbbpy)(C≡CC$_6$H$_5$)$_2$ (**3**)[16] have been reported previously.

Synthesis of Pt(dbbpy)(C≡CC$_6$H$_4$BMes$_2$)$_2$ (1). To a 100 mL Schlenk flask with a stir bar and condenser was added *p*-(dimesitylboryl)phenylacetylene (143 mg, 0.408 mmol, 2.2 equiv), dichloro(dbbpy)platinum(II) (99 mg, 0.185 mmol, 1.0 equiv), CuI (8 mg, 0.041 mmol, 0.1 equiv), and 55 mL of degassed tetrahydrofuran (THF)/triethylamine (NEt$_3$) (10:1, v/v). The mixture was heated to reflux under N_2 for 16 h, then concentrated in vacuo, and partitioned between CH_2Cl_2 and water. The aqueous layer was further extracted with 2 × 30 mL of CH_2Cl_2, dried with $MgSO_4$, filtered, and concentrated to 5 mL with the appearance of a brown precipitate. This was then further purified by column chromatography on silica (benzene) to afford compound 1 as an orange powder. (188 mg, 87%). ^{1}H NMR (400 MHz, C_6D_6): δ 9.60 (d, br, J = 4.7 Hz, 2H, bipy), 7.90 (d, J = 7.9 Hz, 4H, −Ph−), 7.82 (d, J = 8.1 Hz, 4H, −Ph−), 7.59 Hz (s, br, 2H, bipy), 6.92 (s, 8H, Mes), 6.61 (d, J = 4.7 Hz, 2H, bipy), 2.32 (s, 12H, Mes), 2.31 (s, 24H, Mes), 1.09 (s, 18H, *t*-Bu). ^{13}C NMR (100 MHz, C_6D_6): δ 162.1, 156.7, 150.4, 143.2, 142.5, 141.1, 138.6, 137.1, 134.2, 132.0, 128.8, 128.2, 127.9, 124.2, 119.8, 35.4, 30.1, 23.9, 21.3. Anal. Calcd for $C_{70}H_{76}B_2N_2Pt$: C, 72.35; H, 6.59; N, 2.41. Found: C, 72.38; H, 6.55; N, 2.25. Single crystals of **1**·4CH_2Cl_2 were dried under a vacuum prior to analysis, although they may contain residual solvent.

Synthesis of Pt(dppp)(C≡CC$_6$H$_4$BMes$_2$)$_2$ (2). **2** was prepared similarly to **1**, using *p*-(dimesitylboryl)phenylacetylene (135 mg, 0.386 mmol, 2.2 equiv), Pt(dppp)Cl$_2$ (119 mg, 0.175 mmol, 1.0 equiv), CuI (7 mg, 0.039 mmol, 0.1 equiv), and 55 mL of degassed THF/NEt$_3$ (10:1, v/v). The mixture was purified by column chromatography on silica (hexanes and then CH_2Cl_2) and then concentrated in vacuo to afford compound **2** as a white powder (129 mg, 56%). ^{1}H NMR (400 MHz, acetone-d_6): δ 7.95 (m, br, 8H, dppp), 7.42 (m, 8H, dppp), 7.40 (m, 4H, dppp), 7.14 Hz (d, J = 7.2 Hz, 4H, −Ph−), 6.78 (s, 8H, Mes), 6.77 (d, J = 7.2 Hz, 4H, −Ph−), 2.81 (m, 2H, dppp), 2.78 (m, 4H, dppp), 2.24 (s, 12H, Mes), 1.93 (s, 24H, Mes). ^{13}C NMR (100 MHz, acetone-d_6): δ 142.9, 142.5, 141.2, 139.1, 136.65, 134.6, 132.9, 132.2, 131.3, 129.7, 129.1, 128.9, 115.1, 110.6, 26.1, 23.6, 21.2, 20.7. ^{31}P NMR (162 MHz, acetone-d_6): δ −5.26 (t, 2P, J_{P-Pt} = 1088.9 Hz). Anal. Calcd for $C_{79}H_{78}B_2P_2Pt$: C, 72.65; H, 6.02. Found: C, 72.68; H, 6.04.

Single-Crystal X-ray Diffraction Analysis. Single crystals of **1**·4CH_2Cl_2 were obtained from a CH_2Cl_2/hexanes solution, while those of **2**·toluene were obtained from toluene/hexanes. Data were collected on a Bruker AXS Apex II single-crystal X-ray diffractometer with graphite-monochromated Mo Kα radiation, operating at 50 kV and 30 mA at 180 K. Data were processed on a PC with the aid of the Bruker *SHELXTL* software package (version 6.14)[17] and corrected for absorption effects. All structures were solved by direct methods. The crystal lattice of **1** contains four CH_2Cl_2 solvent molecules per molecule of **1**, while the lattice of **2** contains three toluene molecules per molecule of **1**. All solvent molecules were modeled and refined successfully. All non-hydrogen atoms were refined anisotropically. The positions of the hydrogen atoms were calculated, and their contributions in structure

dx.doi.org/10.1021/ic102349h |*Inorg. Chem.* 2011, 50, 3447–3457

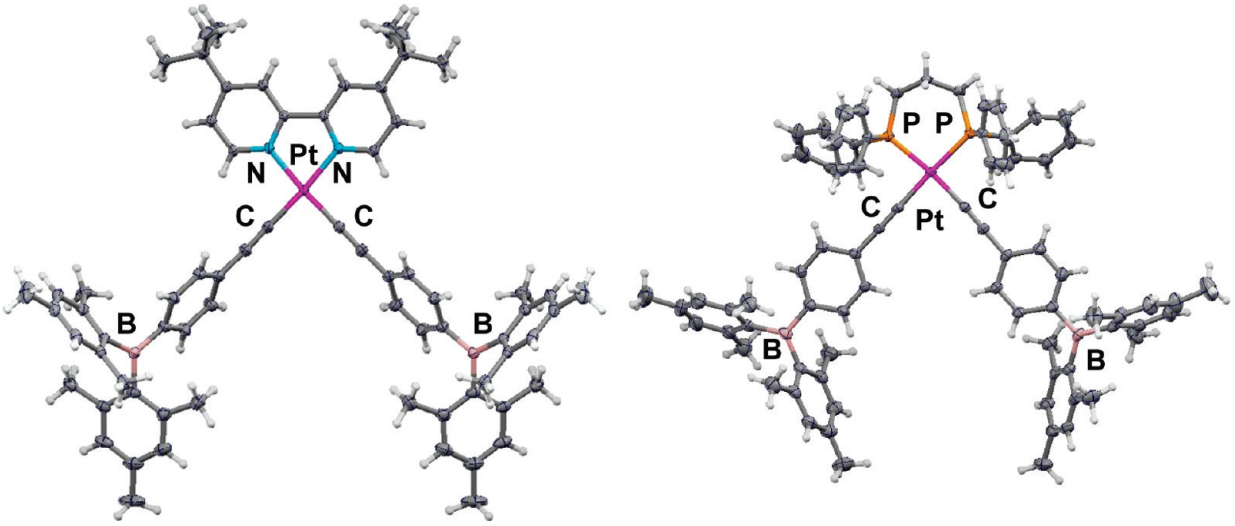

Figure 1. Left: structure of **1** [Pt−C = 1.939(4) Å, Pt−N = 2.060(3) Å; C−Pt−N = 175.33(14)°]. Right: structure of **2** [Pt−P = 2.2898(14) and 2.2900(15) Å; Pt−C = 2.009(6) and 2.017(6) Å; C−Pt−P = 173.79(16) and 175.96(16)°].

factor calculations were included. The crystal structural data of **1**·4CH_2Cl_2 and **2**·toluene have been deposited at the Cambridge Crystallographic Data Centre as CCDC 797877 and 797878, respectively.

Solid-State NMR. Solid-state NMR spectra were acquired using a Varian Infinity Plus console and a 9.4 T Oxford magnet at resonance frequencies of 399.7 MHz for ^{1}H, 128.3 MHz for ^{11}B, 100.5 MHz for ^{13}C, 85 MHz for ^{195}Pt, and 61.4 MHz for ^{2}H. Samples studied include neat **1** (solid, amorphous samples without adsorption of VOCs) and samples of **1** exposed to CH_2Cl_2, benzene, and hexane vapors in a sealed chamber for a minimum of 8 h. The samples were packed in 4-mm-o.d. zirconia rotors sealed with airtight Teflon caps. All solid-state NMR experiments were conducted using a Varian/Chemagnetics 4 mm HX MAS probe. Bloch-decay magic-angle-spinning (MAS) experiments were used for ^{1}H NMR spectra and were referenced to the signal from solid adamantane under MAS at $\delta_{iso}(^1H)$ = 1.85 ppm. 90°−τ_1−180°−τ_2−acq echo experiments using 1.5 μs selective 90° pulse lengths (3.0 μs refocusing pulses) were used to acquire ^{11}B NMR spectra of samples under stationary and MAS conditions, and high-power continuous-wave (CW) ^{1}H decoupling was used during the acquisition period ($\nu_2 \approx$ 50 kHz); spectra were referenced using the signal of liquid $F_3B{\cdot}O(C_2H_5)_2$ at $\delta_{iso}(^{11}B)$ = 0 ppm. ^{13}C NMR spectra were acquired using ^{1}H−^{13}C variable-amplitude cross-polarization (VACP) MAS experiments,[18−20] with high-power ($\nu_2 \approx$ 50 kHz), two-pulse, phase-modulated ^{1}H decoupling;[21] spectra were referenced to the high-frequency peak of solid adamantane under MAS at $\delta_{iso}(^{13}C)$ = 38.56 ppm.[22] The ^{13}C homonuclear double-quantum-filtered spectrum was acquired with the $SR26^{11}_4$ pulse sequence applied at an MAS rate of 9.615 kHz using an experimentally optimized power level (found to be near the theoretical 62.5 kHz);[23,24] VACP preparation was used, and ^{1}H decoupling ($\nu_2 \approx$ 50 kHz) was applied only during signal acquisition, not during the dipolar recoupling period.[25] ^{2}H NMR spectra were acquired using 90°−τ_1−90°−τ_2−acq echo experiments with 3.5 or 4.4 μs pulse lengths, 40 μs interpulse delays, and high-power CW ^{1}H decoupling ($\nu_2 \approx$ 50 kHz) during acquisition. ^{195}Pt NMR spectra of the sample of **1**·4CH_2Cl_2 were acquired using the WURST-CPMG protocol;[26−28] three subspectra were collected 150 kHz apart, using a 10 kHz spikelet spacing and 10 μs WURST pulses swept from +500 to −500 kHz and using a maximum radio-frequency power corresponding to a nutation rate of ca. 75 kHz. For neat **1**, C_6H_6@**1**, and hexanes@**1**, ^{1}H−^{195}Pt CP/CPMG experiments[29,30] were used instead of the direct WURST-CPMG method; 12 subspectra were collected 40 kHz apart, using a 10 kHz spikelet spacing and 6.0 μs ^{195}Pt 180° pulses. All ^{195}Pt NMR spectra were referenced using the signal from a 1 M aqueous solution of Na_2PtCl_6 at $\delta_{iso}(^{195}Pt)$ = 0 ppm.[31,32] Simulated spectra were generated with *WSOLIDS*,[33] for static spectra and *SIMPSON*[34] for MAS spectra.

RESULTS AND DISCUSSION

Syntheses. **1** and **2** can be readily synthesized by a copper (I)-catalyzed transmetalation reaction using 2 equiv of *p*-(dimesitylboryl)phenylacetylene with the appropriate platinum(II) dichloride. **3** can be prepared analogously, using previously reported procedures.[16] These complexes can then be purified by column chromatography and isolated in high yield. **1** is a very robust molecule with excellent stability under ambient conditions in both the solution and solid state, while **2** decomposes slowly under air. Both compounds have been fully characterized by NMR, elemental analyses, and single-crystal X-ray diffraction.

Crystal Structures. Single crystals of **1**·4CH_2Cl_2 and **2**·toluene for X-ray diffraction analyses were obtained by slow evaporation from CH_2Cl_2/hexanes and toluene/hexanes, respectively, and the structures are shown in Figure 1. The Pt−C bonds in **1**·4CH_2Cl_2 are significantly shorter than those in **2** because of the greater *trans* effect of the phosphine chelate. Both compounds form crystal lattices with large voids, as evidenced by the large amount of solvent incorporated into both structures: four CH_2Cl_2 molecules per molecule of **1** and three toluene molecules per molecule of **2**. While many of the previously reported platinum bipyridine acetylide derivatives form either extended pseudolinear or dimeric antiparallel stacked structures in the solid state, with either short Pt···Pt distances (<5 Å) or bipyridyl π−π stacking (<4 Å), neither arrangement is observed for **1**·4CH_2Cl_2. Instead, the Pt(II) square planes of these molecules are oriented at approximately 75° with respect to each other, with the shortest intermolecular Pt···Pt distance being greater than 12 Å and the shortest π−π distances being ∼5.7 Å (Figure 2). Similarly, in the crystal lattice of **2**·toluene (Figure 3), these planes are arranged nearly perpendicularly to one another, and the shortest Pt···Pt distance is ∼7.5 Å.

dx.doi.org/10.1021/ic102349h |*Inorg. Chem.* 2011, 50, 3447–3457

Electronic and Photophysical Properties. **1** is brightly phosphorescent in the solid state and solution ($\Phi = 0.73$ in CH_2Cl_2). The absorption spectrum of **1** shows a low-energy band at 407 nm in CH_2Cl_2, accompanied by a much more intense absorption at 357 nm. These transitions can be unambiguously assigned as a MLCT to the bipyridine group and a ligand-centered (LC) transition on the boron ligand, respectively. This is supported by the absorption spectra of control compounds **2** and **3**, which possess only the LC and MLCT states, respectively (Figure 4). CV experiments further establish that the LUMO of **1** is centered on the bipyridine chelate because the first reduction peak of this compound is very similar to that of **3**. In contrast, **2** undergoes reduction at a much more negative potential typical of triarylboranes (Table 1). Density functional theory (DFT) calculations further establish that the HOMOs for **1**−**3** are dominated by the acetylene π and Pt d orbitals, while the LUMO is located on the bipyridine chelate in **1** and **3** and the boron ligands in **2**, with the orbitals from the boron ligands comprising the LUMO+3 and LUMO+4 in **1** [see the Supporting Information (SI), Figure S7]. Therefore, **1** can be characterized as having two main electronic excited states: the lower-energy (MLCT) state centered on the bipyridine chelate and a higher-energy (LC) state arising from the boron ligands.

In CH_2Cl_2, **1** displays a bright and featureless yellow phosphorescence peak at 541 nm, which is similar to that of **3** and attributable to MLCT phosphorescence. In contrast, **2** displays a weak phosphorescence band with well-resolved vibrational features at 498 nm, due to emission from the LC state on the triarylboron acetylide ligands (Figure 4). The absorption and emission spectra of **1** both show negative solvatochromism typical of the polar ground state in Pt(II) complexes, although the blue shift in the absorption spectrum is much greater for the low-energy MLCT band (50 nm) than the intense LC band (10 nm) from hexanes to CH_2Cl_2. Similarly, the emission spectrum shows a 25 nm blue shift from hexanes to CH_2Cl_2. In contrast, the emission spectrum of **2** shows only a small blue shift with increasing solvent polarity (9 nm from hexane to CH_2Cl_2; see the SI). In both cases, the shape of the emission band does not change significantly with the solvent. Hence, we can conclude that the origin of the electronic transitions in solution remains MLCT for **1** and LC for **2** for all of the solvents that we investigated; however, a remarkably different phenomenon was observed in the solid state.

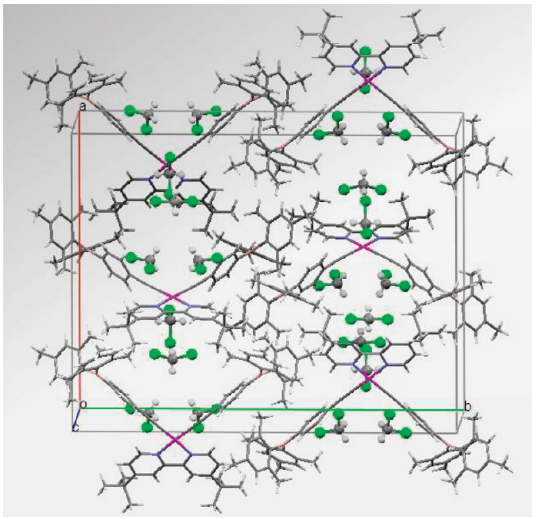

Figure 2. Unit cell packing diagram of $\mathbf{1}\cdot 4CH_2Cl_2$ showing the locations of the CH_2Cl_2 solvent molecules.

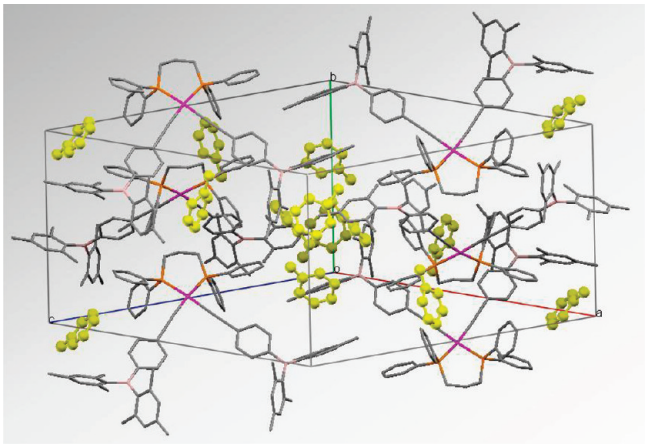

Figure 3. Unit cell packing diagram of **2**·toluene. Toluene solvent molecules are shown in yellow. Hydrogen atoms are omitted for clarity.

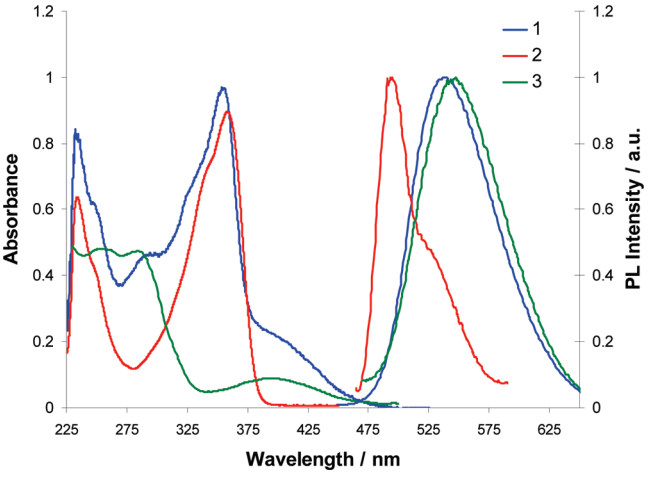

Figure 4. Absorption and normalized emission spectra of **1**−**3** at 10^{-5} M CH_2Cl_2 at 298 K.

Table 1. Photophysical Properties of 1−3

		solution[a]/solid emission, 298 K		
compound	absorption, λ_{max}, nm (ε, 10^4 cm^{-1} M^{-1})[a]	λ_{max} (nm) of CH_2Cl_2/solid	Φ_P[b]	$E_{1/2}^{red}$ (V)[c]
1	248 (6.10), 357 (9.55), 407 (2.00)	541/559	0.73	−1.78
2	236 (6.22), 360 (8.87)	496/496	0.002	−2.26
3	256 (4.81), 286 (4.73), 386 (0.89)	548/535	0.51	−1.80

[a] Measured in CH_2Cl_2 at 1×10^{-5} M. [b] In CH_2Cl_2 solution: relative to $Ir(ppy)_3$ ($\Phi = 0.97$ in 2-MeTHF),[10] ± 10%. [c] In DMF relative to $FeCp_2^{0/+}$.

dx.doi.org/10.1021/ic102349h |*Inorg. Chem.* 2011, 50, 3447–3457

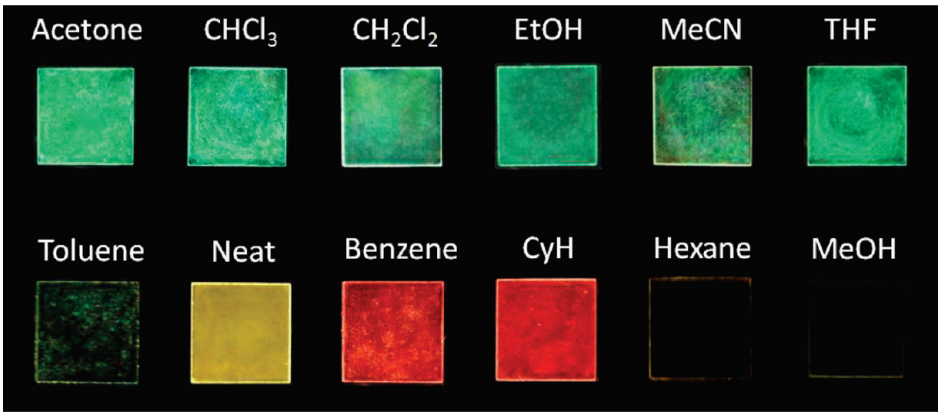

Figure 5. Response of films of **1** under UV irradiation to various organic vapors.

Vapochromism. While **1** and **2** are both capable of acting as selective chemical sensors for fluoride and cyanide anions in solution in the same manner as that of previously reported triarylboranes (see the SI, Figure S3), **1** alone shows reversible vapochromism upon exposure to organic vapors. Both **1** and **2** are luminescent in the solid state under UV irradiation, with emission energies similar to those in a CH_2Cl_2 solution (Table 1). When solid or neat films of **1** are exposed to VOCs, however, the absorption and emission colors of the sample are observed to shift according to the nature of the VOC, producing a response in a matter of seconds (Figure 5). These luminescent changes are reversible either by application of a vacuum or by dissolution and recasting of the film and are persistent in the presence of the detected VOC. The original color of the sample can also be restored upon extended standing under air or mild heating to remove solvent vapor.

Many polar solvents, such as CH_2Cl_2, $CHCl_3$, CH_3CN, acetone, THF, and EtOH, induce an emission color shift from yellow (λ_{max} = 559 nm) to green (λ_{max} = 490−500 nm). This is highly unusual because application of a variety of very different solvent molecules induces the same response. In contrast, application of benzene, cyclohexane, or 1,4-dioxane vapors switches the emission color to red, with the appearance of a new broad emission peak at λ_{max} = 580−620 nm. Because dioxane contains oxygen donor atoms and yet has a dielectric constant similar to that of benzene, the observation of a red shift suggests that the solvent polarity is the key factor in determining the emission shift. Interestingly, exposure to linear hydrocarbons or methanol quenches the emission of the sample entirely. Toluene was also observed to produce green emission, although the vapors were found to readily wet powder films of **1**, making solid-state studies difficult. It should be noted, however, that a similar green emission peak was present in the predominantly red emission spectra of benzene or cyclohexane-treated films of **1**. When **1** is placed in the presence of multiple solvents simultaneously, the effect of polar solvents such as CH_2Cl_2 that turn the sample green appears to be favored.

This switch to green upon exposure to polar solvent vapors may be explained as a solvent-induced inversion of the lowest-energy excited state, from an MLCT transition to a LC transition. Upon exposure to vapors such as CH_2Cl_2, the emission energy and band shape of **1** shifts, closely resembling that of **2**, which emits from a ^{3}LC state with or without VOCs (Figure 6). This suggests that the emissions from neat **2** and **1** after exposure to polar solvents have a common origin. This can be attributed primarily to a change in the MLCT level of **1**, as evidenced by solid-state absorption spectra of powdered films taken before and after exposure to VOCs. The absorption spectrum of a neat film of **1** closely resembles that observed in solution, but once VOCs such as CH_2Cl_2 are added, the MLCT band shifts to higher energy until obscured by the intense LC band.

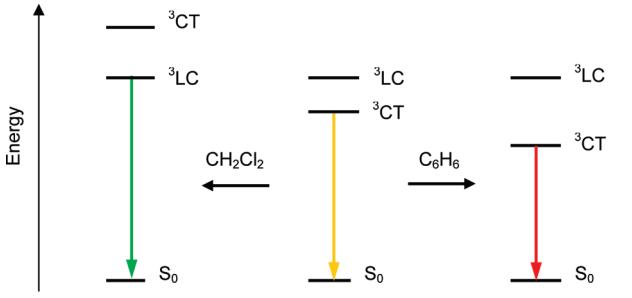

Figure 6. Impact of excited-state level modulation on the emission colors of **1**, using CH_2Cl_2 and benzene as representative examples.

Inversion of the charge-transfer (CT) and LC excited-state energy levels due to solvent polarity has recently been demonstrated in solution-based systems by Castellano and co-workers for platinum(II) bipyridine diacetylide complexes with energetically proximate triplet CT (^{3}CT) and ^{3}LC states.[35,36] They have shown that the energy of the ^{3}CT state can be modulated by the solvent polarity, leaving the ^{3}LC energy relatively unaffected. Pt(II) complexes are well-known to display negative solvatochromism because of large ground-state dipole moments, giving CT excited states that increase in energy with the solvent polarity.[1,2] By variation of the polarity of the solvent, it is thus possible to alter the energy gap between the ^{3}CT and ^{3}LC states by modulation of the ^{3}CT energy level, thereby altering the degree of mixing between the two excited states. In this way, the lowest-energy excited state from which the complex emits can be "inverted", from ^{3}CT in nonpolar media to ^{3}LC in polar media. However, the same "excited-state inversion" phenomenon has not been observed in the solid state previously. Our observations indicate that the vapochromic response of **1** to polar VOCs such as CH_2Cl_2 is due to such excited-state inversion and represents the first observation of this phenomenon in solid-state systems. Conversely, nonpolar solvents such as benzene and cyclohexane appear to reduce the ^{3}CT energy, shifting the emission color to red. Highly nonpolar solvents such as linear hydrocarbons reduce this energy further still, giving a ^{3}CT state so low in energy that vibronic quenching becomes dominant and rendering the sample nonemissive. These processes are outlined in Figure 6.

dx.doi.org/10.1021/ic102349h |*Inorg. Chem.* 2011, 50, 3447–3457

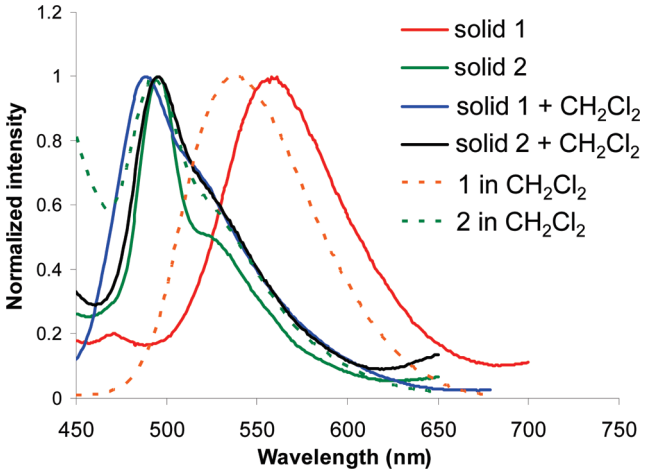

Figure 7. Comparison of the emission spectral change of **1** upon exposure to CH_2Cl_2 in the solid state with that of **2**. The solution spectra for both compounds in CH_2Cl_2 are also shown.

Interestingly, a similar response is observed for methanol vapor. Fluorescence quenching by methanol in various systems was known previously.[37] In the case of **1**, the quenching of luminescence by methanol in the solid state may be due to the introduction of many closely spaced energy levels, which readily facilitate vibronic relaxation. Nonetheless, the fact that a similar excited-state inversion was not observed for **1** in solution remains peculiar. It is likely that the localized dipole−dipole interactions between a molecule of **1** and guest solvent molecules occupying a specific region of free volume in the solid state differ substantially from the interactions between **1** and the continuously changing dipoles of the bulk solution.

PXRD and Solid-State NMR Studies. In most previously reported Pt(II)-based vapochromic systems, the change in the luminescence energy is a direct result of differences in the degree of intermolecular stacking involving the Pt(II) centers or, more rarely, $\pi-\pi$ interactions.[1,2] However, the crystal structure of $\mathbf{1}\cdot 4CH_2Cl_2$ contains no close contacts between the square-planar Pt(II) units (all Pt−Pt distances >12 Å). Furthermore, molecular modeling using two molecules of **1** (from the $\mathbf{1}\cdot 4CH_2Cl_2$ crystal structure) suggests that the steric bulk of the *tert*-butyl and dimesitylboron groups is inconsistent with close intermolecular contacts between the platinum atoms or the bipyridine rings, particularly because **1** has little conformational flexibility. To further investigate the origin of vapochromism in **1**, we examined this system using multinuclear solid-state NMR spectroscopy (SSNMR) and PXRD. Neat **1** as well as samples of **1** exposed to the vapors of CH_2Cl_2, C_6H_6, and hexanes (termed solvent@**1** below) were studied as representative of systems featuring the yellow, green, red, and quenched luminescent states, respectively (Figure 7).

PXRD patterns collected from neat **1** and from each VOC treatment are shown in Figure 8. It is immediately apparent that the structure of CH_2Cl_2@**1** matches that determined in the above single-crystal diffraction study of $\mathbf{1}\cdot 4CH_2Cl_2$, and we will therefore identify this material as $\mathbf{1}\cdot 4CH_2Cl_2$ below. Apart from the lower resolution, the diffraction patterns of neat **1**, C_6H_6@**1**, and hexanes@**1** are very similar to that of $\mathbf{1}\cdot 4CH_2Cl_2$, indicating that the structures of all four materials must be similar. The broadened diffraction peaks in these latter three materials are indicative of reduced long-range ordering, as compared to $\mathbf{1}\cdot 4CH_2Cl_2$. This

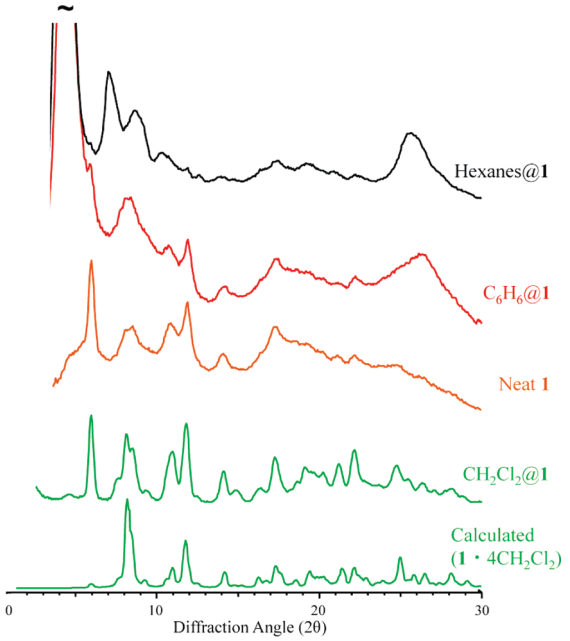

Figure 8. PXRD patterns measured after exposure of **1** to selected solvent vapors.

reduction in long-range ordering may explain our inability to obtain X-ray-quality single crystals from other solvents despite repeated attempts. It is possible that the combination of low conformational flexibility and the complicated molecular shape of **1** prevents stacking without void spaces, unless secondary molecules of suitable size and properties are present; these void spaces would, of course, provide a mechanism for reducing long-range order. The most important conclusion that can be drawn from these data is that there is only a minimal structural reorganization accompanying the vapochromism of **1**. Changes in metallophilic contacts can, therefore, be ruled out as the source of the vapochromic behavior in this system because the crystal structure of $\mathbf{1}\cdot 4CH_2Cl_2$ would require a significant reorganization to bring the Pt(II) moieties together; furthermore, this conclusion is entirely consistent with the SSNMR data presented below.

SSNMR seems an obvious choice to characterize such solid systems but, to our knowledge, has only been applied in two related studies: the tetracyanoplatinum and tetracyanopalladium double salts of platinum tetraarylisonitriles with limited data.[1j,k] The results presented below demonstrate the utility of multinuclear SSNMR for investigating vapochromic materials.

First, ^1H and ^{13}C NMR spectra are used to demonstrate that the solvent molecules are incorporated in each material. Variable-temperature ^2H NMR spectra of deuterated solvent molecules are then used to comment on their motion within the material, which is important for a complete description of how their presence induces the color changes. Next, changes in the host molecules of **1** upon absorption of each vapor are studied directly via the use of ^{195}Pt and ^{11}B NMR.

SSNMR of Guest Solvent Molecules. Displayed in Figure 9 are ^1H and ^{13}C MAS SSNMR spectra of the four preparations of **1**. The changes in the ^{13}C NMR spectral resolution with sample preparation mimic those of the PXRD patterns and are consistent with a higher degree of crystallinity in $\mathbf{1}\cdot 4CH_2Cl_2$ than in the other forms. Aside from resolution changes, the vapor absorption causes only minor changes in the isotropic chemical shifts of

dx.doi.org/10.1021/ic102349h |*Inorg. Chem.* 2011, 50, 3447–3457

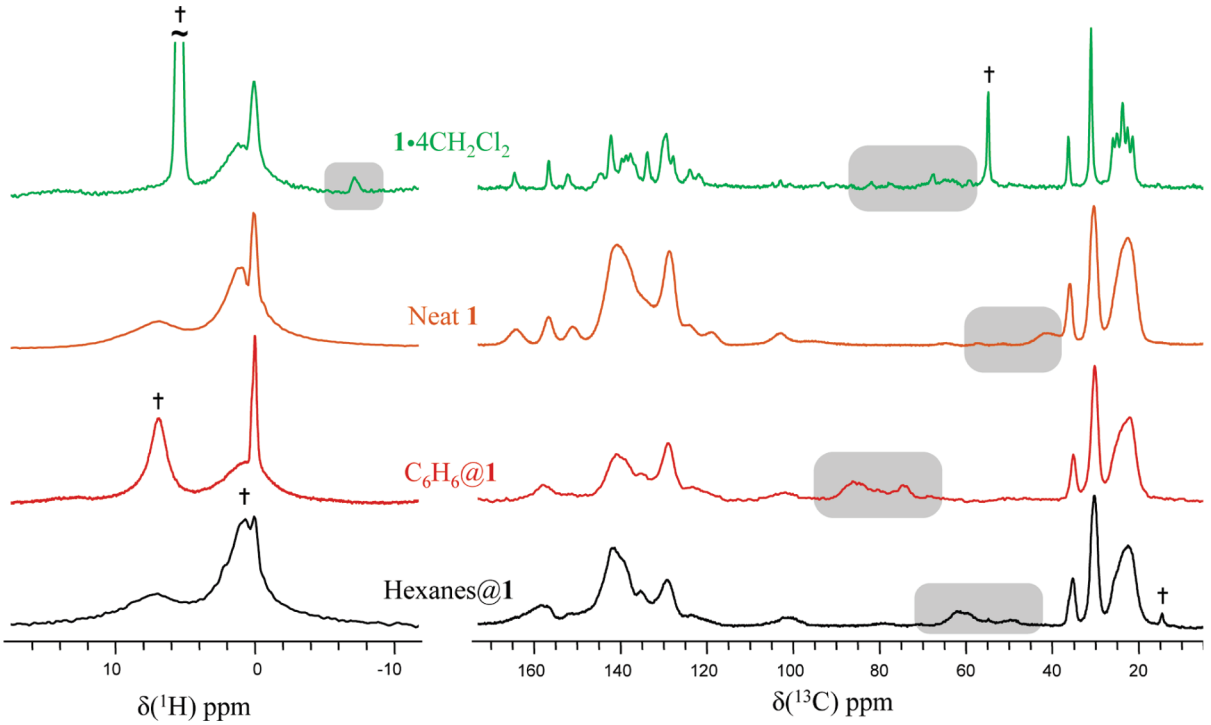

Figure 9. ^{1}H and ^{13}C MAS SSNMR spectra of samples of **1** exposed to selected VOC vapors. Spinning sidebands are marked with gray boxes, and NMR peaks from the incorporated solvents are each marked with a dagger. The spectra were acquired at MAS rates of 7.5 kHz for **1**·4CH_2Cl_2, 10 kHz for neat **1**, 5.5 kHz for C_6H_6@**1**, and 11 kHz (^{1}H NMR spectrum)/8 kHz (^{13}C NMR spectrum) for hexanes@**1**.

the host material **1**, consistent with the behavior displayed in ^{13}C MAS NMR spectra of the vapochromic double salts of [Pt(arylisocyanide)$_4$][Pd(CN)$_4$] and [Pt(arylisocyanide)$_4$][Pt(CN)$_4$].[1j,k] Both ^{1}H and ^{13}C isotropic chemical shifts are similar to those reported above from the solution NMR measurements of **1**. NMR peaks from the absorbed VOCs are readily observed in both ^{1}H and ^{13}C NMR spectra (a second experiment using ^{13}C-labeled benzene, not shown, was necessary to distinguish the solvent peak from the crowded aromatic region in C_6H_6@**1**). Because the intensity of the ^{1}H solvent peaks are of the same order as those from **1**, these spectra demonstrate conclusively that the vapochromic behavior of **1** is accompanied by absorption of the VOCs into the matrix, as opposed to them simply acting as agents of structural change. Interestingly, the distinct changes observed in the ^{13}C NMR spectrum after exposure to CH_2Cl_2 show that the sample is completely converted to the solvate form (**1**·4CH_2Cl_2) in this case.

An attempt was made to probe the proximity of the various ^{13}C nuclei in **1** to guest ^{13}C-labeled benzene molecules using the $SR26_4^{11}$ homonuclear correlation experiment;[23,24] however, the spectrum (not shown) did not contain correlation peaks more intense than the background of natural-abundance ^{13}C spin pairs. It is possible that the large chemical shift anisotropies of the aromatic carbon atoms for which recoupling was attempted and/or the motion of the benzene molecules (vide infra) serve to drastically reduce the efficiency of the dipolar recoupling.[38]

^{2}H NMR experiments conducted over a range of temperatures can be utilized to gain information on the nature of these dynamics by modeling the spectra using well-known techniques.[39−42] Thus, we conducted quadrupolar echo experiments (i.e., 90°−τ_1−90°−τ_2−acq) to record ^{2}H NMR spectra of CD_2Cl_2 and C_6D_6 molecules incorporated into **1**, in the temperature range +40 to −120 °C (Figure 10). Given the low melting point of CH_2Cl_2, it is not surprising that the spectra of **1**·4CH_2Cl_2 from ambient temperature to −40 °C are dominated by a narrow peak, indicative of a rapid isotropic motion of the solvent molecules. Furthermore, the spectra demonstrate that solvent motion is not completely stopped at −120 °C because the line shape expected from a distribution of stationary molecules with the known quadrupolar parameters is not observed.[43]

Numerous publications have featured studies of deuterated benzene as a guest molecule in various types of porous materials, where it has been shown that the ^{2}H NMR spectrum of benzene undergoing rapid jumps about its C_6 rotational axis is characterized by an approximate 70 kHz splitting.[44−52] The ^{2}H NMR spectrum of C_6H_6@**1** at −140 °C displays a quadrupole-perturbed powder pattern with a splitting of 66 kHz, which is assigned to benzene molecules undergoing the aforementioned rapid in-plane rotations. As the temperature is raised, an increasing fraction of the benzene molecules are undergoing rapid isotropic motion, contributing to the narrow peak in the center of the spectrum. Even at the highest temperature investigated, +40 °C, the presence of a quadrupole-perturbed powder pattern is observed, indicating that a portion of the benzene molecules are still undergoing restricted motion; i.e., these molecules do not undergo isotropic motion that is rapid on the NMR time scale ($1/C_Q \approx 5\ \mu s$).[46] Notably, the transition from isotropic to anisotropic motional regimes occurs over a broad temperature range, and none of the spectra is indicative of a mixture of the two types of motion; such behavior is typical of disordered materials in which a range of activation energies are present[47,53] and is, therefore, consistent with the PXRD and other NMR measurements of C_6H_6@**1** (cf. the behavior[46,52] in uniform, crystalline materials).

dx.doi.org/10.1021/ic102349h |*Inorg. Chem.* 2011, 50, 3447–3457

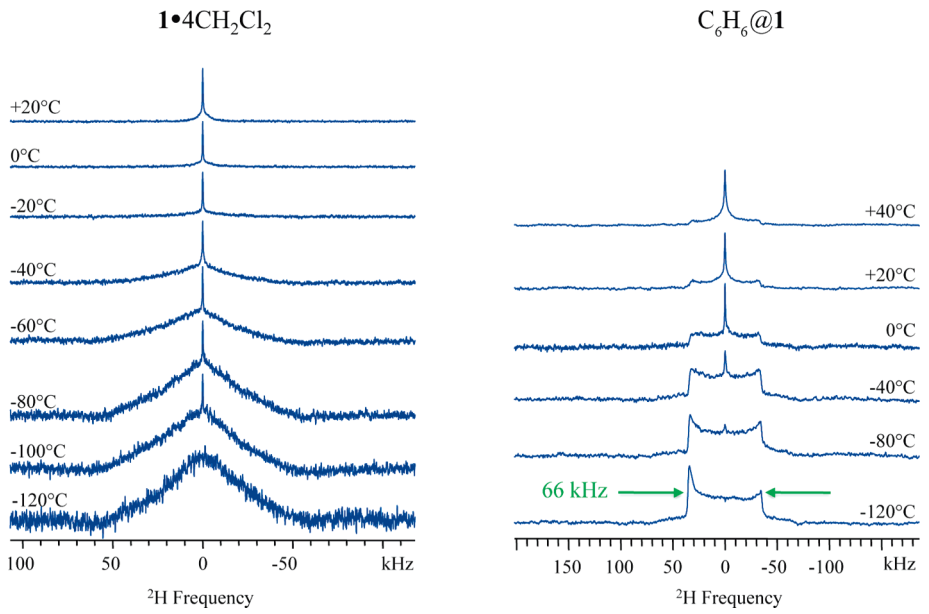

Figure 10. Variable-temperature ^{2}H NMR spectra of $\mathbf{1}\cdot 4CH_2Cl_2$-$d_2$ and C_6H_6-d_6@**1**.

For approximately 50% of the benzene molecules at ambient temperature, the isotropic mode of motion is slow on the NMR time scale and is, therefore, also slow on the time scale of the optical spectroscopy (the lifetimes of the electronic excited states were measured to be ≤ 2 μs). The two-component line shape apparent in the ambient-temperature ^{2}H NMR spectrum of $\mathbf{1}\cdot 4CH_2Cl_2$ demonstrates that a significant fraction of the CH_2Cl_2 molecules are also undergoing restricted motion (a quantitative measure of this fraction would require extensive experimentation given that the longitudinal and transverse relaxation rate constants are likely different in the two motional regimes, and each may, furthermore, mirror the structural heterogeneity of the sample). It is therefore possible that the vapor-induced color changes in **1** are accompanied by directional interactions between the guest VOCs and host molecules of **1**.

SSNMR of the Host Material. Because the platinum atom is central to the phosphorescent emission of **1**, the effects of VOC absorption were also studied using ^{195}Pt SSNMR. Before the experimental results are discussed, a brief description is given on the well-known but often underexploited relationship between optically excited transitions and the nuclear magnetic shielding (NMS) measured using NMR; this relationship also extends to the chemical shift (CS) because this is simply the difference in NMS from a reference compound (the relationships between the NMS and CS have been discussed lucidly elsewhere).[32,54] The NMS of a nucleus is due to a small local magnetic field induced by a large external magnetic field and can be expressed using the familiar expressions of time-independent perturbation theory, as was first done by Ramsey.[55−57] Only the paramagnetic shielding term is described herein because it is responsible for nearly all of the differences in magnetic shielding between chemical environments. External-field-perturbed MOs, which are similar to the zero-field MOs except that they contain some admixture of virtual (unoccupied) orbitals, are the source of the response magnetic field. The amount that a particular virtual orbital mixes into a particular occupied orbital, and therefore the NMS contribution from that occupied/virtual MO pair, is inversely dependent on the energy gap

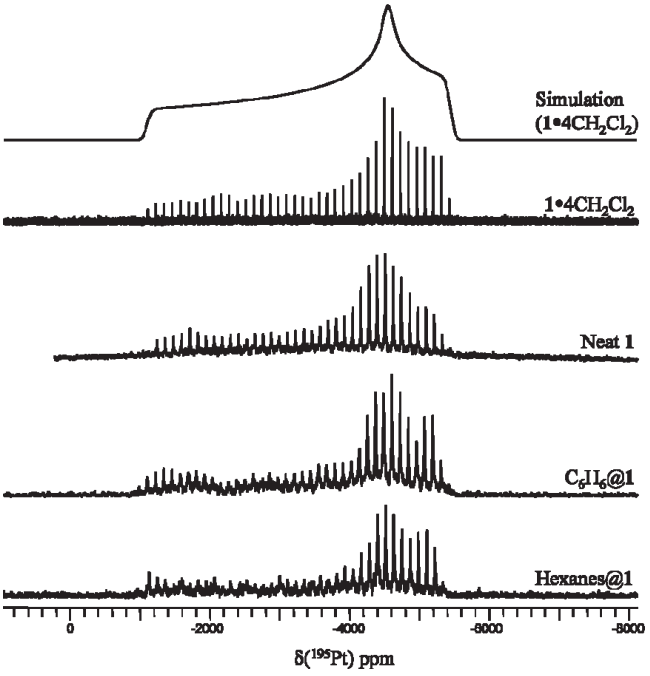

Figure 11. ^{195}Pt SSNMR static spectra of samples of **1** exposed to vapors of selected VOCs.

between the two MOs. In addition, each MO pair's influence on the magnetic shielding depends on its degree of localization near the nucleus of interest, as well as on its shape, determined by its constituent atomic orbitals.[57−59] The NMS is therefore dependent on a large array of occupied/virtual MO energy spacings in the valence level, while optical spectroscopy probes some of these same energy spacings one at a time. Because the color changes observed in **1** must arise from solvent-induced energy shifts in the real and/or virtual MO involved in a particular optical absorption, the Pt CS tensor should change if the MO that shifts is localized near Pt.

dx.doi.org/10.1021/ic102349h |*Inorg. Chem.* 2011, 50, 3447–3457

Table 2. ^{195}Pt CS Tensors Measured from Samples of 1 Exposed to the Vapors of Selected VOCs[a]

material	δ_{11}	δ_{22}	δ_{33}	δ_{iso}	Ω	κ
1·4CH_2Cl_2	−1100(100)	−4550(50)	−5450(100)	−3700(100)	4350(200)	−0.59(3)
neat **1**	−1150(100)	−4450(200)	−5300(200)	−3600(200)	4150(300)	−0.59(10)
C_6H_6@**1**	−1000(100)	−4600(200)	−5350(200)	−3650(200)	4350(300)	−0.66(10)
hexanes@**1**	−1000(100)	−4550(200)	−5350(200)	−3600(200)	4350(300)	−0.63(10)

[a] Values for the CS tensor elements are derived using line-shape simulations and are given here using the convention $\delta_{11} \geq \delta_{22} \geq \delta_{33}$. An alternate representation of the CS tensor is also included for convenience: isotropic shift, $\delta_{iso} = 1/3(\delta_{11} + \delta_{22} + \delta_{33})$; span, $\Omega = \delta_{11} - \delta_{33}$; skew, $\kappa = 3(\delta_{22} - \delta_{iso})/\Omega$ $(-1 \leq \kappa \leq 1)$.[66] Spectral simulations are consistent with the experimental line shapes within the ranges given in brackets for the principal components.

The ^{195}Pt SSNMR spectra of neat **1** and each vapor-treated sample are displayed in Figure 11. Under the conditions used (stationary samples, high-power ^{1}H decoupling, etc.), the powder pattern depends only on the Pt CS tensors, which are given in Table 2. It should be noted that the signal-to-noise ratios of these spectra were increased by acquiring a train of echoes, Fourier transformations of which yield the "spikelet" spectra shown, as in a CPMG-type experiment.[29,30] These spikelet peaks trace out the classic CSA-dominated patterns (Figure 11). The 400 kHz broad spectrum from **1**·4CH_2Cl_2 was acquired using only three subspectra by making use of the broad excitation bandwidth of frequency-swept WURST pulses. The transverse relaxation of the ^{195}Pt nuclei was found to be slightly more efficient in the other three samples, so cross-polarization (CP) from ^{1}H was used instead of direct excitation. The lower bandwidth of the CP method required the acquisition of many more subspectra (12 vs 3), but this was balanced by the signal enhancement of CP, making the total acquisition time ca. 24 h for all of the spectra in Figure 11.

Isotropic Pt CSs are known to span a range of ca. 15000 ppm, and the present results are at the lower end of the +5000 to −5000 ppm range typical for Pt(II) compounds.[60,61] The CS tensors observed for neat **1**, **1**·4CH_2Cl_2, C_6H_6@**1**, and hexanes@**1** are characterized by large spans (Ω > 4000 ppm), as is typical for square-planar Pt(II) compounds; for example, Ω = 3472 ppm in (cod)PtI_2,[62] and the largest span published to date is for K_2PtCl_4, where Ω = 10500 ppm.[61,63−65] The CS tensors are each characterized by a skew value near −1 and likely have an orientation similar to that proposed for a series of (η^2-1,5-cyclooctadiene)PtX_2 (X = I or Cl) and other related Pt(II) materials, with δ_{11} perpendicular to the rectangular plane.[62] The most notable feature apparent in the data of Figure 11 and Table 2 is that the ^{195}Pt CS tensor of neat **1** is not measurably different from those of the three solvent-exposed forms. From this evidence and the above discussion of the relationship between MOs and the CS tensor, we conclude that the vapochromic behavior of **1** does not involve changes in the MOs localized on Pt. Clearly, there can be no Pt−Pt stacking in any of the preparations of **1** because the metal−metal interactions would lead to Pt-localized MOs significantly different from those in **1**·4CH_2Cl_2. The solid-state NMR data therefore indicate, in agreement with the PXRD measurements and molecular modeling, that changes in Pt−Pt interactions are not responsible for the vapochromic behavior of **1**.

The invariant ^{195}Pt NMR spectra of **1** as well as PXRD data rule out modulations in the structure that involve Pt−Pt interactions. The nonpolar VOC benzene reduces the MLCT energy, allowing this optical pathway to dominate. In contrast, the polar VOC CH_2Cl_2 increases the energy of the MLCT by stabilizing the polar ground state of the molecule to the point that the LC transition (localized on the triarylboron moiety) becomes the lowest-energy excited state and the source of the observed phosphorescence. The ground state of **1**, as in **3**, has a strong electric dipole moment, and because the MLCT transition is opposite to the orientation of the ground-state dipole moment[35] and smaller in magnitude, more polar VOCs cause the MLCT tranisition to shift to higher energy. This inverse solvatochromic effect induces excited-state switching, as demonstrated by Castellano and others for similar dual-chromophore compounds in liquid solutions.[35]

To further rule out chromophore−chromophore contacts as the cause of the unique vapochromic effect observed, ^{11}B SSNMR spectra of the stationary and MAS samples of **1**·4CH_2Cl_2 and C_6H_6@**1** were acquired. Because the boron atom is a distinct moiety central to the LC transition, looking for changes in the CS and electric-field-gradient tensors is another way to examine possible chromophore−chromophore interactions in the solid state induced by solvent uptake into the void space of **1**. Both the CS and EFG tensors, determined using line-shape simulations, are found to be similar to those of trimesitylborane (see S8 of the Supporting Information for spectra and further details).[38] The ^{11}B NMR spectra of **1**·4CH_2Cl_2 and C_6H_6@**1** are completely indistinguishable, demonstrating that the boron environment is unaltered by absorption of these VOCs. While the boron atom in **1** is shown above to be accessible by small anions, the steric crowding at this site ensures that there is no close contact with the much larger VOC molecules. Small amounts of impurities from repeated cycling in a liquid solvent over a long period of time are seen in each spectrum; however, these impurities could not be removed because of the small amount of sample remaining for these final experiments. While these impurities hinder a complete determination of the NMR parameters, they do not affect the conclusions noted above.

CONCLUSIONS

In summary, the first example of a triarylboron-functionalized platinum(II) acetylide compound that displays distinct luminescent responses to a variety of VOCs in the solid state has been presented. ^{1}H and ^{13}C SSNMR spectroscopies were was used to directly observe adsorption of solvent into **1**, and ^{195}Pt SSNMR results discount Pt−Pt metallophilic interactions as being responsible for the response to VOCs. On the basis of optical and NMR spectroscopic data, we conclude that (1) the vapochromic response of **1** toward polar solvents such as CH_2Cl_2 is caused by inversion of the lowest-energy excited state from ^{3}MLCT to ^{3}LC

dx.doi.org/10.1021/ic102349h |Inorg. Chem. 2011, 50, 3447–3457

in the solid state because of an increase in the MLCT level, (2) a decrease in the ^{3}MLCT level is responsible for the shift in the emission color to red upon exposure to benzene/cyclohexanes, and (3) the quenching response obtained by the treatment of **1** with linear hydrocarbons or methanol is likely due to the introduction of many closely spaced energy levels, which readily facilitate vibronic relaxation. Because ^{11}B and ^{195}Pt NMR spectra show no changes upon exposure to VOCs, we postulate that interactions between adsorbed solvent molecules and the bipyridine chelate are likely responsible for changes in the MLCT level, though it remains unclear why a similar effect is not observed in solution. This study demonstrates that metal−metal or $\pi-\pi$ stacking interactions between molecules of the sensor are not necessary for a vapochromic response and that interactions between the sensor and VOC analyte can indeed be sufficient.

■ ASSOCIATED CONTENT

Supporting Information. Solution NMR spectra for **1** and **2**, additional absorption/emission spectra, CV diagrams, DFT results, F^- and CN^- titration data for **1** and **2**, ^{11}B SSNMR spectra of **1**, and crystal structural data for **1** and **2**. This material is available free of charge via the Internet at http://pubs.acs.org.

■ AUTHOR INFORMATION

Corresponding Author

*E-mail: suning.wang@chem.queensu.ca (S.W.), rschurko@uwindsor.ca (R.W.S.).

■ ACKNOWLEDGMENT

The authors gratefully acknowledge the Natural Sciences and Engineering Research Council of Canada for financial support. R.W.S. also acknowledges the Canadian Foundation for Innovation, the Ontario Innovation Trust, and the University of Windsor for funding the solid-state NMR facility and the Ontario Ministry of Research and Innovation for an Early Researcher Award.

■ REFERENCES

(1) (a) Kato, M.; Omura, A.; Toshikawa, A.; Kishi, S.; Sugimoto, Y. *Angew. Chem.* **2002**, *114*, 3315. (b) Lu, W.; Chan, M. C. W.; Zhu, N.; Che, C.-M.; He, Z.; Wong, K.-Y. *Chem.—Eur. J.* **2003**, *9*, 6155. (c) Ni, J.; Zhang, L.-Y.; Wen, H.-M.; Chen, Z.-N. *Chem. Commun.* **2009**, 3801. (d) Ni, J.; Wu, Y.-H.; Zhang, X.; Li, B.; Zhang, L.-Y.; Chen, Z.-N. *Inorg. Chem.* **2009**, *48*, 10202. (e) Kato, M.; Kishi, S.; Wakamatsu, Y.; Sugi, Y.; Osamura, Y.; Koshiyama, T.; Hasegawa, M. *Chem. Lett.* **2005**, *34*, 1368. (f) Buss, C. E.; Anderson, C. E.; Pomije, M. K.; Lutz, C. M.; Britton, D.; Mann, K. R. *J. Am. Chem. Soc.* **1998**, *120*, 7783. (g) Buss, C. E.; Mann, K. R. *J. Am. Chem. Soc.* **2002**, *124*, 1031. (h) Kunugi, Y.; Miller, L. L.; Mann, K. R.; Pomije, M. K. *Chem. Mater.* **1998**, *10*, 1487. (i) Daws, C. A.; Exstrom, C. L; Sowa, J. R., Jr.; Mann, K. R. *Chem. Mater.* **1997**, *9*, 363. (j) Exstrom, C. R.; Sowa, J. R., Jr.; Daws, C. A.; Janzen, D.; Mann, K. R.; Moore, G. A.; Stewart, F. F. *Chem. Mater.* **1995**, *7*, 15. (k) Isbester, P. K.; Zalusky, A.; Lewis, D. H.; Douskey, M. C.; Pomije, M. J.; Mann, K. R.; Munson, E. *J. Catal. Today* **1999**, *49*, 363.

(2) (a) Du, P.; Schneider, J.; Brennessel, W. W.; Eisenberg, R. *Inorg. Chem.* **2008**, *47*, 69. (b) Wadas, T. J.; Wang, Q.-M.; Kim, Y.; Flaschenreim, C.; Blanton, T. N.; Eisenberg, R. *J. Am. Chem. Soc.* **2004**, *126*, 16841. (c) Grove, L. J.; Oliver, A. G.; Krause, J. A.; Connick, W. B. *Inorg. Chem.* **2008**, *47*, 1408. (d) Grove, L. J.; Rennekamp, J. M.; Jude, H.; Connick, W. B. *J. Am. Chem. Soc.* **2004**, *126*, 1594. (e) Lu, W.; Chan, M. C. W.; Cheung, K.-K.; Che, C. M. *Organometallics* **2001**, *20*, 2477. (f) Field, J. S.; Grimmer, C. D.; Munro, O. Q.; Waldron, B. P. *Dalton Trans.* **2010**, *39*, 1558. (g) Albrecht, M.; van Koten, G. *Adv. Mater.* **1999**, *11*, 171 and references cited therein. (h) Matsumoto, K.; Sakai, K. *Adv. Inorg. Chem.* **1999**, *49*, 375. (i) Kitagawa, S.; Uemura, K. *Chem. Soc. Rev.* **2005**, *34*, 109.

(3) (a) Katz, M. J.; Ramnial, T.; Yu, H. Z.; Leznoff, D. B. *J. Am. Chem. Soc.* **2008**, *130*, 10662. (b) Lefebvre, J.; Batchelor, R. J.; Leznoff, D. B. *J. Am. Chem. Soc.* **2004**, *126*, 16117. (c) Luquin, A.; Elosúa, C.; Vergara, E.; Estella, J.; Cerrada, E.; Bariáin, C.; Matías, I. R.; Garrido, J.; Laguna, M. *Gold Bull.* **2007**, *40*, 225. (d) Bariáin, C.; Matías, I. R.; Romeo, I.; Garrido, J.; Laguna, M. *Sens. Actuators* **2001**, *B76*, 25. (e) Balch, A. L. *Struct. Bonding (Berlin)* **2007**, *123*, 1. (f) Rawashdeh-Omary, M. A.; Omary, M.; Fackler, J. P., Jr.; Galassi, R.; Pietroni, B. R.; Brurini, A. *J. Am. Chem. Soc.* **2001**, *123*, 9689. (g) Yam, V. W.-W.; Cheng, E. C.-C. *Chem. Soc. Rev.* **2008**, *37*, 1806.

(4) Pang, J.; Marcotte, E. J.-P.; Seward, C.; Brown, R. S.; Wang, S. *Angew. Chem., Int. Ed.* **2001**, *40*, 4042.

(5) (a) Hudson, Z. M.; Wang, S. *Acc. Chem. Res.* **2009**, *42*, 1584. (b) Tanaka, D.; Takeda, T.; Chiba, T.; Watanabe, S.; Kido, J. *Chem. Lett.* **2007**, *36*, 262. (c) Jäkle, F. *Chem. Rev.* **2010**, *110*, 3985. (d) Jäkle, F. *Coord. Chem. Rev.* **2006**, *250*, 1107. (e) Entwistle, C. D.; Marder, T. B. *Angew. Chem., Int. Ed.* **2002**, *41*, 2927. (f) Entwistle, C. D.; Marder, T. B. *Chem. Mater.* **2004**, *16*, 4574. (g) Lam, S.-T.; Zhu, N.; Yam, V. W.-W. *Inorg. Chem.* **2009**, *48*, 9664.

(6) (a) Noda, T.; Shirota, Y. *J. Am. Chem. Soc.* **1998**, *120*, 9714. (b) Noda, T.; Ogawa, H.; Shirota, Y. *Adv. Mater.* **1999**, *11*, 283. (c) Shirota, Y.; Kinoshita, M.; Noda, T.; Okumoto, K.; Ohara, T. *J. Am. Chem. Soc.* **2000**, *122*, 1102. (d) Shirota, Y. *J. Mater. Chem.* **2005**, *15*, 75. (e) Doi, H.; Kinoshita, M.; Okumoto, K.; Shirota, Y. *Chem. Mater.* **2003**, *15*, 1080. (f) Jia, W.-L.; Bai, D.-R.; McCormick, T.; Liu, Q.-D.; Motala, M.; Wang, R.; Seward, C.; Tao, Y.; Wang, S. *Chem.—Eur. J.* **2004**, *10*, 994. (g) Jia, W.-L.; Moran, M. J.; Yuan, Y.-Y.; Lu, Z. H.; Wang, S. *J. Mater. Chem.* **2005**, *15*, 3326. (h) Jia, W.-L.; Feng, X.-D.; Bai, D.-R.; Lu, Z.-H.; Wang, S.; Vamvounis, G. *Chem. Mater.* **2005**, *17*, 164. (i) Li, F.-H.; Jia, W.-L.; Wang, S.; Zhao, Y.-Q.; Lu, Z.-H. *J. Appl. Phys.* **2008**, *103*, 034509.

(7) (a) Collings, J. C.; Poon, S. Y.; Droumaguet, C. L.; Charlot, M.; Katan, C.; Pålsson, L. O.; Beeby, A.; Mosely, J. A.; Kaiser, H. M.; Kaufmann, D.; Wong, W.-Y.; Blanchard-Desce, M.; Marder, T. B. *Chem.—Eur. J.* **2009**, *15*, 198. (b) Yuan, Z.; Taylor, N. J.; Ramachandran, R.; Marder, T. B. *Appl. Organomet. Chem.* **1996**, *10*, 305. (c) Yuan, Z.; Entwistle, C. D.; Collings, J. C.; Albesa-Jové, D.; Batsanov, A. S.; Howard, J. A. K.; Kaiser, H. M.; Kaufmann, D. E.; Poon, S.-Y.; Wong, W.-Y.; Jardin, C.; Fathallah, S.; Boucekkine, A.; Halet, J. F.; Taylor, N. J.; Marder, T. B. *Chem.—Eur. J.* **2006**, *12*, 2758.

(8) (a) Wade, C. R.; Broomsgrove, A. E. J.; Aldridge, S.; Gabbaï, F. P. *Chem. Rev.* **2010**, *110*, 3958 and references cited therein. (b) Hudnall, T. W.; Chiu, C.-W.; Gabbaï, F. P. *Acc. Chem. Res.* **2009**, *42*, 388.

(9) (a) Zhou, G. J.; Ho, C. L.; Wong, W.-Y.; Wang, Q.; Ma, D.-G.; Wang, L.-X.; Lin, Z.-Y.; Marder, T. B.; Beeby, A. *Adv. Funct. Mater.* **2008**, *18*, 499. (b) Hudson, Z. M.; Sun, C.; Helander, M. G.; Amarne, H.; Lu, Z.-H.; Wang, S. *Adv. Funct. Mater.* **2010**, *20*, 3426.

(10) Sajoto, T.; Djurovich, P. I.; Tamayo, A. B.; Oxgaard, J.; Goddard, W. A.; Thompson, M. E. *J. Am. Chem. Soc.* **2009**, *131*, 9813.

(11) O'Boyle, N. M.; Tenderholt, A. L.; Langner, K. M. *J. Comput. Chem.* **2008**, *29*, 839.

(12) Frisch, M. J. et al. *Gaussian 03*, revision C.02; Gaussian, Inc.: Wallingford, CT, 2004.

(13) An, Z.; Odom, S. A.; Kelley, R. F.; Huang, C.; Zhang, X.; Barlow, S.; Padilha, L. A.; Fu, J.; Webster, S.; Hagan, D. J.; Van Stryland, E. W.; Wasielewski, M. R.; Marder, S. R. *J. Phys. Chem. A* **2009**, *113*, 5585.

(14) Huertas, S.; Hissler, M.; McGarrah, J. E.; Lachicotte, R. J.; Eisenberg, R. *Inorg. Chem.* **2001**, *40*, 1183.

(15) Annibale, G.; Bortoluzzi, M.; Marangoni, G.; Pitteri, B. *Transition. Met. Chem.* **2005**, *30*, 748.

(16) Hissler, M.; Connick, W. B.; Geiger, D. K.; McGarrah, J. E.; Lipa, D.; Lachicotte, R. J.; Eisenberg, R. *Inorg. Chem.* **2000**, *39*, 447.

(17) *SHELXTL*, version 6.14; Bruker AXS: Madison, WI, 2000−2003.

(18) Pines, A.; Waugh, J. S.; Gibby, M. G. *J. Chem. Phys.* **1972**, *56*, 1776.

(19) Pines, A.; Gibby, M. G.; Waugh, J. S. *J. Chem. Phys.* **1973**, *59*, 569.
(20) Peersen, O. B.; Wu, X. L.; Kustanovich, I.; Smith, S. O. *J. Magn. Reson., Ser. A* **1993**, *104*, 334.
(21) Bennett, A. E.; Rienstra, C. M.; Auger, M.; Lakshmi, K. V.; Griffin, R. G. *J. Chem. Phys.* **1995**, *103*, 6951.
(22) Earl, W. L.; Vanderhart, D. L. *J. Magn. Reson.* **1982**, *48*, 35.
(23) Kristiansen, P. E.; Carravetta, M.; Lai, W. C.; Levitt, M. H. *Chem. Phys. Lett.* **2004**, *390*, 1.
(24) Kristiansen, P. E.; Carravetta, M.; van Beek, J. D.; Lai, W. C.; Levitt, M. H. *J. Chem. Phys.* **2006**, *124*, 234510.
(25) Marin-Montesinos, I.; Brouwer, D. H.; Antonioli, G.; Lai, W. C.; Brinkmann, A.; Levitt, M. H. *J. Magn. Reson.* **2005**, *177*, 307.
(26) Bhattacharyya, R.; Frydman, L. *J. Chem. Phys.* **2007**, *127*, 8.
(27) O'Dell, L. A.; Schurko, R. W. *Chem. Phys. Lett.* **2008**, *464*, 97.
(28) O'Dell, L. A.; Rossini, A. J.; Schurko, R. W. *Chem. Phys. Lett.* **2009**, *468*, 330.
(29) Hung, I.; Rossini, A. J.; Schurko, R. W. *J. Phys. Chem. A* **2004**, *108*, 7112.
(30) Siegel, R.; Nakashima, T. T.; Wasylishen, R. E. *J. Phys. Chem. B* **2004**, *108*, 2218.
(31) Harris, R. K.; Reams, P.; Packer, K. J. *J. Chem. Soc., Dalton Trans.* **1986**, *5*, 1015.
(32) Harris, R. K.; Becker, E. D.; De Menezes, S. M. C.; Goodfellow, R.; Granger, P. *Pure Appl. Chem.* **2001**, *73*, 1795.
(33) Eichele, K.; Wasylishen, R. E. *WSOLIDS*, 2.0.18; University of Alberta: Edmonton, Alberta, Canada, 2000.
(34) Bak, M.; Rasmussen, J. T.; Nielsen, N. C. *J. Magn. Reson.* **2000**, *147*, 296.
(35) (a) Goeb, S.; Rachford, A. A.; Castellano, F. N. *Chem. Commun.* **2008**, 814. (b) Pomestchenko, I. E.; Castellano, F. N. *J. Phys. Chem. A* **2004**, *108*, 3485. (c) She, C.; Rachford, A. A.; Wang, X.; Goeb, S.; El-Ballouli, A. O.; Castellano, F. N.; Hupp, J. T. *Phys. Chem. Chem. Phys.* **2009**, *11*, 8586. (d) McGarrah, J. E.; Hupp, J. T.; Smirnov, S. N. J. *Phys. Chem. A* **2009**, 113.
(36) (a) Chan, S. C.; Chan, M. C. W.; Wang, Y.; Che, C.-M.; Cheung, K.-K.; Zhu, N. *Chem.—Eur. J.* **2001**, *7*, 4180. (b) McGarrah, J. E.; Eisenberg, R. *Inorg. Chem.* **2003**, *42*, 4355. (c) Wadas, T. J.; Chakraborty, S.; Lachicotte, R. J.; Wang, Q.-M.; Eisenberg, R. *Inorg. Chem.* **2005**, *44*, 2628.
(37) Gryczynski, I.; Lakowicz, J. R. *Photochem. Photobiol.* **1995**, *62*, 426.
(38) Bryce, D. L.; Wasylishen, R. E.; Gee, M. *J. Phys. Chem. A* **2001**, *105*, 3633.
(39) Spiess, H. W. *J. Chem. Phys.* **1980**, *72*, 6755.
(40) Greenfield, M. S.; Ronemus, A. D.; Vold, R. L.; Vold, R. R.; Ellis, P. D.; Raidy, T. E. *J. Magn. Reson.* **1987**, *72*, 89.
(41) Chandrakumar, N. *Spin-1 NMR*; Springer-Verlag: Berlin, 1996.
(42) Vold, R. L.; Hoatson, G. L. *J. Magn. Reson.* **2009**, *198*, 57.
(43) Minott, G. L.; Ragle, J. L. *J. Magn. Reson.* **1976**, *21*, 247.
(44) Meirovitch, E.; Belsky, I.; Vega, S. *J. Phys. Chem.* **1984**, *88*, 1522.
(45) Eckman, R. R.; Vega, A. J. *J. Phys. Chem.* **1986**, *90*, 4679.
(46) Ok, J. H.; Vold, R. R.; Vold, R. L.; Etter, M. C. *J. Phys. Chem.* **1989**, *93*, 7618.
(47) Schulz, M.; Vanderest, A.; Rossler, E.; Kossmehl, G.; Vieth, H. M. *Macromolecules* **1991**, *24*, 5040.
(48) Xiong, J. C.; Maciel, G. E. *J. Phys. Chem. B* **1999**, *103*, 5543.
(49) Aksnes, D. W.; Kimtys, L. *Appl. Magn. Reson.* **2002**, *23*, 51.
(50) Gedat, E.; Schreiber, A.; Albrecht, J.; Emmler, T.; Shenderovich, I.; Findenegg, G. H.; Limbach, H. H.; Buntkowsky, G. *J. Phys. Chem. B* **2002**, *106*, 1977.
(51) Trezza, E.; Grassi, A. *Macromol. Rapid Commun.* **2002**, *23*, 260.
(52) Villanueva-Garibay, J. A.; Muller, K. *J. Phys. Chem. B* **2004**, *108*, 15057.
(53) Gedat, E.; Schreiber, A.; Albrecht, J.; Emmler, T.; Shenderovich, I.; Findenegg, G. H.; Limbach, H. H.; Buntkowsky, G. *J. Phys. Chem. B* **2002**, *106*, 1977.
(54) Harris, R. K.; Becker, E. D.; De Menezes, S. M. C.; Granger, P.; Hoffman, R. E.; Zilm, K. W. *Pure Appl. Chem.* **2008**, *80*, 59.
(55) Ramsey, N. F. *Phys. Rev.* **1950**, *78*, 699.
(56) Jameson, C. J. In *Multinuclear NMR*, 1st ed.; Mason, J., Ed.; Plenum Press: New York, 1987.
(57) Autschbach, J.; Ziegler, T. In *Encyclopedia of Nuclear Magnetic Resonance*; Grant, D. M., Harris, R. K., Eds.; John Wiley and Sons: Chichester, U.K., 2002; Vol. 9, pp 306−323.
(58) Cornwell, C. D. *J. Chem. Phys.* **1966**, *44*, 874.
(59) Grutzner, J. B. In *Recent Advances in Organic NMR Spectroscopy*; Lambert, J. B., Rittner, R., Eds.; Norell Press: Landisville, PA, 1987; pp 17−42.
(60) Goodfellow, R. J. In *Multinuclear NMR*, 1st ed.; Mason, J., Ed.; Plenum Press: New York, 1987; p 3.
(61) Duncan, T. M. *A Compilation of Chemical Shift Anisotropies*; Farragut Press: Chicago, IL, 1990.
(62) Thibault, M.-H.; Lucier, B. E. G.; Schurko, R. W.; Fontaine, F.-G. *Dalton Trans.* **2009**, 7701.
(63) Keller, H. J.; Rupp, H. H. *Z. Naturforsch., A: Astrophys., Phys. Phys. Chem.* **1970**, *A 25*, 312.
(64) Keller, H. J.; Rupp, H. H. *Z. Naturforsch., A: Astrophys., Phys. Phys. Chem.* **1971**, *A 26*, 785.
(65) Sparks, S. W.; Ellis, P. D. *J. Am. Chem. Soc.* **1986**, *108*, 3215.
(66) Mason, J. *Solid State Nucl. Magn. Reson.* **1993**, *2*, 285.